·Experimental Research·

Protective effect of myricitrin on retinal microvascular endothelial cells induced by high glucose and its regulation mechanism

Liu Qian, Liu Changgeng, Li Haijun, Dong Yangzeng, Zhang Ying Department of Ophthalmology, Henan Provincial People's Hospital, People' s Hospital of Zhengzhou University, Henan Eye Hospital, Henan Eye Institute, Zhengzhou 450003, China

Corresponding author: Liu Qian, Email: qianliuyk@163.com

[Abstract] Objective to explore the effect of myricitrin on the injury of human retinal microvascular endothelial cells (HRMECs) induced by high glucose and its regulation mechanism.

Methods HRMECs were divided into normal control group, high glucose group and 12.5 μg/ml, 25.0 μg/ml and 5 μg/ml myricitrin groups. HRMECs transfected with pcDNA and pcDNA-circZNF292, respectively and then cultured in high-glucose medium containing 25 mmol/L D-glucose for 24 hours were assigned as pcDNA group and pcDNA-circZNF292 group. HRMECs transfected with siR-NC and siR-circZNF292, respectively and then cultured in medium containing 50.0 μg/ml myricitrin and 25 mmol/L D-glucose for 24 hours were assigned as myricitrin + siR-NC group and myricitrin+ siR-circZNE292 group. The cell apoptosis rate was detected by flow cytometry. The concentration of malondialdehyde (MDA) and the activity of superoxide dismutase (SOD) in cells were detected by enzyme-linked immunosorbent assay (ELISA) kits. The expression levels of circZNF292 and miR-23b-3p were detected by real-time fluorescence quantitative PCR. The targeting relationship between circZNF292 and miR-23b-3p was detected by dual luciferase reporter assay. The relative expression levels of B-cell lymphoma-2 (bcl-2) and bcl-2-related X protein (bax) were assayed by Western blot.

Results Significant differences were found in the relative expressions of bax and bcl-2 proteins , cell apoptosis rate, MDA concentration , SOD activity, circZNF292 and miR-23b-3p among normal control group, high glucose group and 12. 5 μg/ml, 25.0 μg/ml, 50.0 μg/ml myricitrin groups (F = 105.707, 111.835, 74.515, 109.651, 135.020, 219.919, 116.304; all at P <0.001). With the increase of myricitrin concentration, the relative expression levels of bax protein, cell apoptosis rate, MDA concentration and miR-23b-3p in cells gradually decreased, while the relative expression levels of bcl-2 protein, SOD activity and circZNF292 increased, with statistically significant differences among groups with different concentrations of myricitrin (all at P < 0. 05). In the co-transfected wild-type (WT) -circZNF292 cells, the relative luciferase activity in miR-23b-3p group was 0. 35 ±0.03, which was lower than 0.96 ±0.09 in microRNA-negative control group, and the difference was statistically significant (t = 11. 137, P <0. 001). Compared with pcDNA group, the relative expression levels of bcl-2 protein, circZNF292 and MDA concentration in cells of pcDNA-circZNF292 group were significantly increased, and the relative expression levels of bax protein, miR-23b-3p, cell apoptosis rate and SOD activity were significantly decreased (all at P <0. 05). The relative expression levels of bax protein, miR-23b-3p, cell apoptosis rate and MDA concentration were reduced and relative expression levels of bcl-2 protein, circZNF292 and SOD activity were enhanced in myricitrin group and myricitrin+siR-NC group in comparison with high glucose group and myricitrin + siR-circZNF292 group, showing statistically significant differences (all at P <0.05).

Conclusions Myricitrin can inhibit cell apoptosis and oxidative stress by regulating the expression of circZNF292/miR-23b-3p, thereby reducing the damage of HRMECs induced by high glucose.

Key words Myricitrin, Apoptosis, Human retinal microvascular endothelial cells, CircZNF292, MiR-23b-3p

Fund program: National Natural Science Foundation of China (U1404812); Provincial Joint Project of Medical Science and Technology Research Program of Henan Province (SBGJ2018083); Basic Research Project of Henan Provincial Eye Hospital (21JCQN005); Talent Project of Henan Provincial People's Hospital 23456

DOI: 10.3760/cma.j.cn115989-20210809-00451

Diabetic retinopathy (DR) is one of the common sight-threatening conditions, which is characterized by retinal vasculopathy and retinal neurodegeneration. It arises from changes in the microenvironment of the retina and its adjacent tissues induced by long-term hyperglycemic conditions. The occurrence and progression of DR are associated with abnormal gene expression and signaling pathway function, which are attributable to high-glucose conditions, tissue hypoxia, oxidative stress injury and chronic inflammatory process[1-3]. Myricitrin is a natural polyphenol hydroxy-flavonoid glycoside flavonoid compound that is mainly distributed in the bark and fruit of Chinese bayberry (Myrica rubra). It has anti-inflammatory and antioxidant effects, which is helpful in inhibiting dopaminergic nerve cell apoptosis and oxidative stress damage in SN4741 mice, and thus delaying the progression of Parkinson's disease[4-7]. Some studies suggested that myricetin derivatives could alleviate oxidative stress injury of retinal pigment epithelial cells induced by hydrogen peroxide[8]. Based on the results from these studies, one may infer that myricitrin is protective against retinal tissue damage arising from DR. However, the specific effect of myricitrin on the retina and its exact mechanism remain unclear. CircRNA (circular RNA) is a non-coding RNA characterized by covalently closed loops. In recent years, an increasing number of studies have showed that circRNA is abnormally expressed in DR, and it may therefore serve as a potential target for DR therapy[9-11]. CircZNF292 expression was up-regulated and may compete with miR-23b-3p (microRNA-23b-3p), which can inhibit lens epithelial cell apoptosis and attenuate cell damage[12-13]. Zhao et al. found that persistent hyperglycemic conditions stimulated miR-23b-3p expression in HRMECs (human retinal microvascular endothelial cells, HRMECs). Conversely, reduced miR-23b-3p expression suppressed cell apoptosis[14]. These findings suggest that circZNF292/miR-23b-3p may play a role in the occurrence and progression of DR. In this context, we aim to explore the protective effect of myricitrin derivatives against HRMECs induced by high glucose condition and its molecular mechanism, with a view to shedding light on the pathogenesis and clinical treatment of DR.

1 Materials and Method

1.1 Materials

1.1.1 Cell sources HRMECS were purchased from ATCC, USA.

1.1.2 The main reagents and instruments Myricitrin (at least 98% purity) was purchased from Shanghai Kang Lang Biological technology co ., LTD; DMEM culture medium and fetal bovine serum (FBS) were purchased from Shanghai Biyuntian Biotechnology Co., LTD; Cell apoptosis detection Kit and luciferase activity detection Kit were purchased from Beijing Soleibao Technology Co., LTD; Malondialedhyde (MDA) and superoxide

dismutase (SOD) detection kit were purchased from Nanjing Jiancheng Bioengineering Institute; Trizol reagent, cDNA synthesis reagent and qRT-PCR kit were purchased from Thermo Fisher, USA; Lipofectamine1™ 3000 transfection reagent was purchased from Invitrogen, USA; miR-NC, miR-23b-3P mimics, pcDNA, pcDNA-circZNF292, siR-circZNF292 and siR-NC were purchased from Shanghai Jima Pharmaceutical Technology Co., LTD; bcl-2 (B-cell lymphoma-2,bcl-2) antibody(sc-7382), bax (bcl-2 associated X protein, bax) antibody (sc-7480) and HRP labeled goat anti-rabbit IgG antibody (sc-69786) were purchased from Santa, USA Cruz Inc. Flow cytometry was purchased from BDC6, Beijing Agos Biotechnology Co., LTD. Gel scanning system was purchased from Gel Doc XR+, Bio-Rad, USA. Nanodrop 2000C UV spectrophotometer was purchased from Thermo Fisher Technologies, USA. Real-time PCR instrument was purchased from 7500, ABI, USA.

1.2 Methods

1.2.1 Cell grouping and culture HRMECs were grown in 96-well plates (3 x10^3 cells/well) and divided into 5 groups: cells in normal control group cultured in DMEM medium with 5.5 mmol/L D-glucose and 10% FBS for 24 hours; cells in high glucose group cultured in DMEM medium with 25 mmol/L D-glucose and 10% FBS for 24 hours; and HRMECs in 12.5 ug/ml, 25.0 ug/ml, 50.0 ug/ml myricitrin groups cultured in high glucose medium consisting of 12.5 ug / ml, 25.0 ug/ml and 50.0 ug/ml myricitrin for 24 h, respectively.

1.2.2 Preparation of transfection solution and cell transfection First, preparation of liposome transfection solution. The concentration of pcDNA, pcDNA-circZNF292, siR-circZNF292 and Sir-NC were diluted to 0.5 μmol/L in the DMEM culture medium without FBS and were incubated at room temperature (RT) for 5 min as solution A. 16 μl Lipofectamine™ 3000 transfection reagent was added to 200 μl DMEM medium without FBS and was well mixed as solution B. Then the mixture of solution A and B was incubated for 20 min at RT. Second, transfecting cells in different groups. The HRMECs were grown in 6-well plates(2x10^5 cells/ml) and divided into high glucose + pcDNA group and high glucose + pcDNA-circZNF292 group. 16 μl liposome-mediated transfection solution was added to 400 μl HRMECs culture medium for 6 h. The normal culture solution was added and cultivated for 48 h after discarding the supernatant. Then HRMECs were divided into two groups to incubate with the transfection mixture (20ul siR NC or siR-circZNF292) for 6 hours, which medium was then changed with normal medium to grow for 48 hours, and these cells were subsequently treated with complete medium containing 50.0ug/ml myricitrin and 25 mmol/L D-glucose for another 24 hours.

1.2.3 Measurement of apoptosis rate using flow cytometry The procedures have previously been described in detail before[15]. Briefly, HRMECs in different groups were digested with 0.25% trypsin, centrifuged at 3000 r/min for 6min, and then washed with cooled PBS (phosphate buffer solution, PBS) after discarding the supernatant. The cells were collected using centrifugation and were resuspended in 500 ul binding buffer before adding 5 ul Annexin-FITC and 5 ul PI. Shaking for 10min in the dark was necessary and apoptosis rate in different groups was detected by flow cytometry.

1.2.4 Detection of MDA concentration and SOD activity using Enzyme linked immunosorbent assay (ELISA) The procedures have previously been described in detail[16]. Briefly, HRMECs treated with trypsin in different groups were lysed by repeated freezing and thawing method to form homogenate. The 0.1ml homogenate was added to a centrifuge tube, followed by adding 0.2ml MDA or SOD solution. To collect supernatant, the mixture was cooled in a water bath and was centrifuged at 1000r/min for 10min at RT. 200ul supernatant, combined with 100 ul working solution, was added to each well in 96-well plates and fully mixed. The sample wells and blank control wells were set up at the same time. The MDA concentration and SOD activity were measured using a microplate reader.

1.2.5 Quantitative evaluation of the relative expression of circZNF292 and miR-23b-3p in HRMECs using real-time fluorescence PCR The procedures have previously been described in detail [17]. Briefly, HRMECs in different groups were collected and added Trizol reagent (1 ml). Total RNA was extracted using a total RNA extraction kit, with a A_{260} /A_{280} ratio of 1.6-1.8. RNA was reverse-transcribed into cDNA, and 2 ul cDNA were subsequently used for amplification (the volume of amplification reaction is 25ul). Reaction conditions were as follows: (1) pre-denaturation at 95°C for 2 min; (2) denaturation at 95-°C for 30 s; (3) annealing at 58°C for 30 s; (4) and extension at 72°C for 30 s. The whole process was performed for a total of 40 cycles. The sequence of circZNF292 forward primers and reverse primer are 5'-GAGACTGGGGTGTGGAAAAA-3' and 5'-CGGGCTTTAACATAACTTTGG-3', while the sequence of miR-23b-3p forward primers and reverse primer are 5'-GGGATCACATTGCCAGGGAT-3' and 5'-CAGTGCGTGTCGTGGAGT-3'. The sequence of GAPDH forward primers and reverse primer are 5'-GGAGCGAGATCCCTCCAAAAT-3' and 5'-GGCTGTTGTCATACTTCTCATGG-3', whereas the sequence of U6 forward primers and reverse primer are 5'-ATTGGAACGATACAGAGAAGATT-3' and 5'-GGAACGCTTCACGAATTTG-3'. Gene amplification of circZNF292 was performed when GAPDH was used as a reference gene. On the other hand, gene amplification of miR-23b-3p was performed when U6 was used as an internal control. $2^{-\Delta\Delta Ct}$ was used to evaluate the relative expression of target genes.

1.2.6 Detection of the targeting relationship between circZNF292 and miR-23b-3p in HRMECs using dual luciferase reporter Starbase was used to predict the binding sites of circZNF292 and miR-23b-3p. The binding sites were cloned into pGL3) plasmids to construct WT (wild type, WT) vector (WT-circZNF292); the MUT (Mutant type, MUT) vector (MUT-circZNF292) was constructed by combining the kit of point mutation with the mutated sites. After that, WT-circZNF292 and MUT-circZNF292 were cotransfected with miR-NC or miR-23b-3p mimics in HRMECs, respectively. After a 48-hour culture, cell luciferase activity was detected using a dual luciferase reporter assay.

1.2.7 Detection of the relative expression of bax and bcl-2 proteins in HRMECs using Western blot The procedures have previously been described in detail[18]. Briefly, HRMECs in different groups were collected, washed with PBS and lysed by 500u1 RIPA lysis buffer to extract the total protein of cells. The concentration of the protein was measured quantitively using a BCA protein assay kit. We took 40 ug protein for SDS-PAGE electrophoresis, transferred the separated protein gel to PVDF membrane before placing it in a 5% skim milk blocking solution for 2 hours at room temperature; bax (1:800), bcl-2 (1:800) primary antibody and GAPDH antibody (1:1000) were added and incubated at 4°C overnight. After PBST rinsing, the corresponding secondary antibody (1:3000) was added and incubated at 37°C for 1 h. EC luminescence was developed with the rinse of PBST. The Quantitative One software was used to analyze the gray value of the protein bands. Moreover, the ratio of the gray value of the target protein and built-in GAPDH protein was represented as the relative expression of the target protein.

1.3 Statistical Methods

All statistical analysis was performed with IBM SPSS software version 21.0 (SPSS Inc, Chicago, IL, USA). Data were confirmed to be normally distributed as per the S-W test and represented as $\bar{x} \pm s$. The differences in the dual luciferase reporter detection results between two groups were compared with independent sample T-test. The overall differences in apoptosis rate, protein expression, MDA concentration and SOD activity among multiple groups were compared using one-way ANOVA analysis combined with LSD-t test. P <0.05 was used as the level of significance.

2 Results

2.1 Comparison of cell apoptosis rate and apoptosis-related gene expression among groups with different concentrations of myricitrin

The gray level of bax protein band was the weakest, while that of bcl-2 protein band was the strongest in the normal control group. Compared with the normal control group, the gray level of bax band was significantly enhanced, while the gray level of bcl-2 band was significantly reduced in the high glucose group. Increasing doses of myricitrin led to decreases in the gray level of bax protein band and increases in the gray level of bcl-2 protein band (Fig. 1). The differences in the relative expression of bax, bcl-2 and apoptosis rate among different groups were statistically significant (F = 105.707, 111.835, 74. 515, all at P < 0.01). Compared with the normal control group, the relative expression of bax and cell apoptosis rate in the high glucose group were significantly increased, while the relative expression of bcl-2 was significantly decreased (P < 0.01). The relative expression of bax and the cell apoptosis rate decreased significantly while the relative expression of bcl-2 increased significantly as the dose of myricitrin increased among groups with different doses of myricitrin (all at P < 0.05) (Fig. 2 and Table 1).

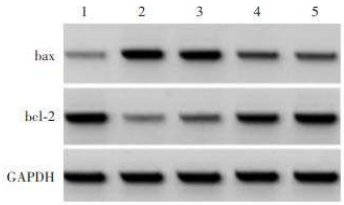

Figure 1 Expression of apoptosis-associated protein in human retinal microvascular endothelial cells (HRMECs) of each group by Western blot 1: normal control group; 2: high glucose group; 3: 12.5 μg/ml myricitrin group; 4: 25.0 μg/ml myricitrin group; 5: 50.0 μg/ml myricitrin group bcl-2: B-cell lymphoma-2; bax: bcl-2 associated X protein

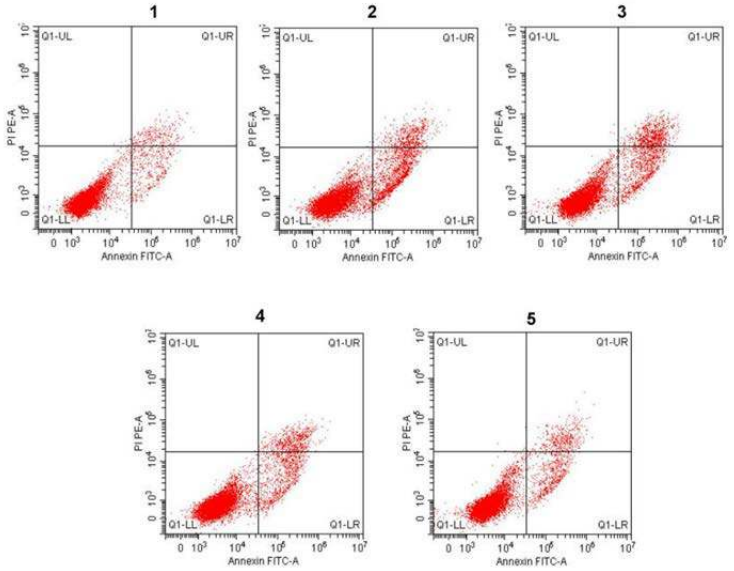

Figure 2 Apoptosis rate among different groups by flow cytometry The apoptotic rate was significantly increased in high glucose group, however, the apoptotic rate reduced as the increase of myricitrin-treated concentrations 1: normal control group 2: high glucose group 3: 12.5 μg/ml myricitrin group 4: 25.0 μg/ml myricitrin group 5: 50.0 μg/ml myricitrin group

Table 1 Comparison of relative expression of apoptotic-association proteins and apoptotic rate among different groups ($\bar{x}\pm s$)

Group	Sample size	bax	bcl-2	Apoptosis rate (%)
Normal control group	3	0.18±0.03	0.80±0.06	7.85±0.71
High glucose group	3	0.71±0.05[a]	0.18±0.02[a]	20.40±1.15[a]
12.5 μg/ml myricitrin group	3	0.55±0.04[b]	0.28±0.04[b]	18.33±1.12[b]
25.0 μg/ml myricitrin group	3	0.36±0.04[bc]	0.51±0.04[bc]	15.30±1.03[bc]
50.0 μg/ml myricitrin group	3	0.23±0.02[bcd]	0.72±0.05[bcd]	10.31±1.22[bcd]
F		105.707	111.835	74.515
P		<0.001	<0.001	<0.001

Note: Compared with respective normal control group, [a]P<0.05; compared with respective high glucose group, [b]P<0.05; compared with respective 12.5 μg/ml myricitrin group, [c]P<0.05; compared with respective 25.0 μg/ml myricitrin group, [d]P<0.05 (One-way ANOVA, LSD-t test) bcl-2: B-cell lymphoma-2; bax: bcl-2 associated X protein

2.2 Comparison of MDA concentration and SOD activity among groups with different doses of myricitrin

There were significant differences in MDA concentration and SOD activity among normal control group, high glucose group and groups with different doses of myricitrin (F = 109. 651,135. 020, all at P < 0.001). Compared with the normal control group, MDA concentration was significantly higher in the high glucose group, but SOD activity was significantly lower (all at P < 0.05). Compared with the high glucose group, MDA concentration among groups with different dose of myricitrin decreased significantly while SOD activity increased significantly in a dose-dependent manner. The differences were statistically significant among groups with different dose of myricitrin (all at P < 0.05) (Table. 2).

Table 2 Comparison of MDA level and SOD activity among different groups ($\bar{x}\pm s$)

Group	Sample size	MDA (mmol/L)	SOD [μmol/(min·L)]
Normal control group	3	124.39±12.02	207.36±12.03
High glucose group	3	350.00±22.39[a]	47.89 ± 4.50[a]
12.5 μg/ml myricitrin group	3	306.07±16.20[b]	80.26 ± 6.55[b]
25.0 μg/ml myricitrin group	3	247.74±12.45[bc]	141.62 ± 9.51[bc]
50.0 μg/ml myricitrin group	3	166.51±11.98[bcd]	173.47±13.42[bcd]
F		109.651	135.020
P		<0.001	<0.001

Note: Compared with respective normal control group, [a]*P*<0.05; compared with respective high glucose group, [b]*P*<0.05; compared with respective 12.5 μg/ml myricitrin group, [c]*P*<0.05; compared with respective 25.0 μg/ml myricitrin group, [d]*P*<0.05 (One-way ANOVA, LSD-*t* test) MDA: malondialedhyde; SOD: superoxide dismutase

2.3 Comparison of relative expression levels of circZNF292 and miR-23b-3p among groups with different concentrations of myricitrin

The relative expressions of circZNF292 and miR-23b-3p in the normal control group, high glucose group and groups with different doses of myricitrin group differed significantly (F = 219.919, 116.304, all at $P < 0.001$). Compared with the normal control group, the relative expression of circZNF292 decreased significantly, while the relative expression of miR-23b-3p increased significantly in the high glucose group (all at $P < 0.05$). Compared with the high glucose group, the relative expression of circZNF292 showed a significant reduction, whereas miR-23b-3p expression showed a significant increase in a dose-dependent manner among groups with different concentrations of myricitrin (all at $P < 0.05$) (Table 3).

Table 3 Comparison of relative expression levels of circZNF292 and miR-23b-3p among different groups ($\bar{x}\pm s$)

Group	Sample size	circZNF292	miR-23b-3p
Normal control group	3	1.00±0.01	1.00±0.06
High glucose group	3	0.25±0.02[a]	2.34±0.10[a]
12.5 μg/ml myricitrin group	3	0.39±0.04[b]	1.89±0.08[b]
25.0 μg/ml myricitrin group	3	0.57±0.04[bc]	1.60±0.06[bc]
50.0 μg/ml myricitrin group	3	0.79±0.05[bcd]	1.36±0.10[bcd]
F		219.919	116.304
P		<0.001	<0.001

Note: Compared with respective normal control group, [a]*P*<0.05; compared with respective high glucose group, [b]*P*<0.05; compared with respective 12.5 μg/ml myricitrin group, [c]*P*<0.05; compared with respective 25.0 μg/ml myricitrin group, [d]*P*<0.05 (One-way ANOVA, LSD-*t* test) miR: microRNA

2.4 Validation of targeting relationship between circZNF292 and miR-23b-3p in HRMECs

Starbase prediction showed the presence of mutual binding sites in the complementary sequence between circZNF292 and miR-23b-3p (Figure 3). The relative luciferase activity values of miR-23b-3p (0.35 ± 0.03) were significantly lower than that of miR-NC (0.96 ± 0.09) in cotransfected WT-circZNF292 cells (t = 11.137, $P < 0.05$). However, there were no significant differences in relative luciferase activity values of miR-23b-3p and miR-NC (0.98 ± 0.08 and 1.00 ± 0.11, respectively) in MUT-circZNF292 cells (t = 0.441, $P > 0.05$).

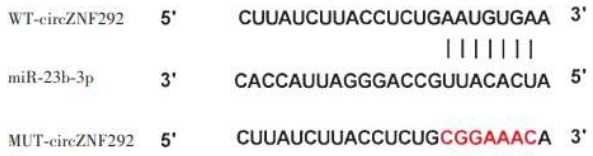

Figure 3 Matching sequences of circZNF292 and miR-23b-3p Starbase prediction showed that there were binding sites between circZNF292 and miR-23b-3p WT: wild type; miR: microRNA; MUT: mutant type

2.5 Comparison of relative expression levels of circZNF292 and miR-23b-3p, cell apoptosis rate and apoptosis-related gene expression among different circZNF292 transfection groups

Compared with the pcDNA group, the relative expression of circZNF292 significantly increased while the relative expression of miR-23b-3p significantly decreased in the pcDNA-circZNF292 group (t = 13.874, 13.668, all at $P < 0.001$). Compared with the pcDNA group, the relative expression of Bax protein and apoptosis rate significantly decreased while the relative expression of bcl-2 protein significantly increased in the pcDNA-circZNF292 group (t = 8.133, 9.046, 13.070, all at P ≤0.001) (Fig. 4, 5 and Table 4).

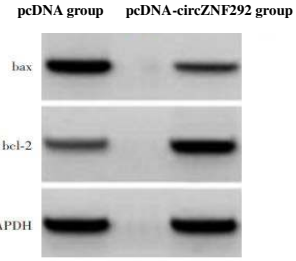

Figure 4 Expression of -associated protein by Western blot in different circZNF292- transfected groups 1: pcDNA group; 2: pcDNA-circZNF292 group Bcl-2: B-cell lymphoma-2; Bax: bcl-2 associated X protein

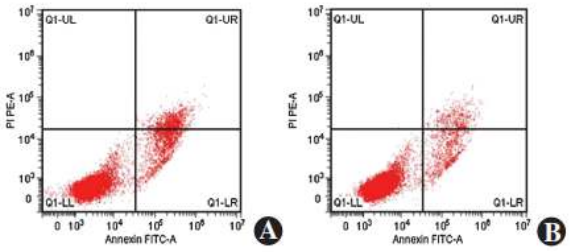

Figure 5 Apoptosis rate in different circZNF292 transfection groups The apoptosis rate of the cells was reduced in pcDNA-circZNF292 group compared with pcDNA group A: pcDNA group B: pcDNA-circZNF292 group

Table 4 Comparison of relative expression levels of circZNF292 and miR-23b-3, apoptosis-associated indexes between different plasmid-transfected groups($\bar{x}\pm s$)

Group	Sample size	circZNF292	miR-23b-3p	Apoptotic rate (%)	bax	bcl-2
pcDNA group	3	1.00±0.02	1.00±0.01	22.63±1.43	0.70±0.08	0.19±0.03
pcDNA-circZNF292 group	3	2.61±0.20[a]	0.52±0.06[a]	13.24±1.09[a]	0.28±0.04[a]	0.63±0.05[a]
t		13.874	13.668	9.046	8.133	13.070
P		<0.001	<0.001	0.001	0.001	<0.001

Note: (Independent samples *t* test) miR: microRNA; bcl-2: B-cell lymphoma-2; bax: bcl-2 associated X protein

2.6 Comparison of MDA concentration and SOD activity among different circZNF292 transfection groups

Compared with the pcDNA group, the MDA concentration showed a significant increase while SOD activity values showed a significant reduction in the pcDNA-circZNF292 group (t = 11. 281,15. 585, all at P < 0. 001) (Table 5).

Table 5 Comparison of MDA concentration and SOD activity between different circZNF292 transfection groups ($\bar{x}\pm s$)

Group	Sample size	MDA (mmol/L)	SOD [μmol/(min·L)]
pcDNA group	3	354.47±21.52	47.82± 5.65
pcDNA-circZNF292 group	3	194.21±11.93[a]	161.20±11.02[a]
t		11.281	15.585
P		<0.001	<0.001

Note: (Independent samples t test) MDA: malondialedhyde; SOD: superoxide dismutase

2.7 Comparison of cell apoptosis among different siRNA transfection groups

The gray level of bax protein band was the highest, whereas that of bcl-2 protein band was the lowest in the high glucose group. The gray scale of bax protein band showed a significant reduction, while the gray scale of bcl-2 protein band showed a significant increase in both myricitrin group and myricitrin + siR-NC group. Compared with the myricitrin group and myricitrin + siR-NC group, the gray scale of bax protein band enhanced while the gray scale of bcl-2 protein band decreased in myricitrin + siR-circZNF292 group (Fig. 6). The relative expressions of circZNF292, miR-23b-3p, bax and bcl-2 and cell apoptosis rate showed significant differences among high glucose group, myricitrin group, myricitrin + siR-NC group and myricitrin + siR-circZNF292 group (F = 163.188, 107.321, 85.623, 59.310, 96.786, all at P < 0.001). The results showed that the relative expressions of bax and miR-23b-3p and cell apoptosis rate were significantly lower, while the relative expressions of circZNF292 and bcl-2 were significantly higher in the myricitrin group and myricitrin + siR-NC group than that of both high glucose group and myricitrin + siR-circZNF292 group (all at P < 0.01) (Fig. 6,7 and Table 6).

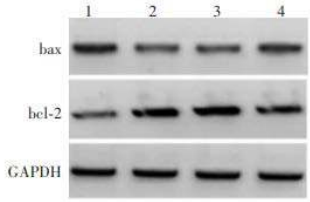

Figure 6 Expression of apoptosis-associated protein by Western blot in different siRNA-transfected groups 1: high glucose group; 2: myricitrin group; 3: myricitrin+siR-NC group; 4: myricitrin+siR-circZNF292 bax: bcl-2 associated X protein; bcl-2: B-cell lymphoma-2

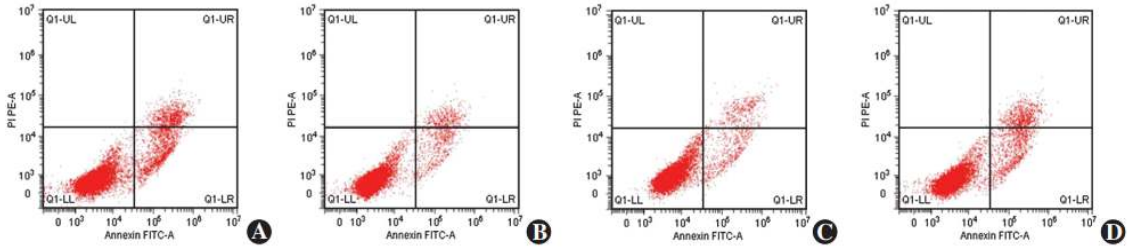

Figure 7 Apoptosis rate by flow cytometry of in different siRNA-transfected groups The apoptotic rate of the cells was reduced in myricitrin group cpmpared with the myricitrin+siR-cirCZNF292 group A: high glucose group B: myricitrin group C: myricitrin+siR-NC group D: myricitrin+siR-circZNF292

Table 6 Comparison of relative expression levels of circZNF292 and miR-23b-3, apoptosis-associated indexes among different siRNA transfection groups ($\bar{x}\pm s$)

Group	Sample size	circZNF292	miR-23b-3p	Apoptotic rate (%)	bax	bcl-2
High glucose group	3	1.00±0.03	1.00±0.01	22.71±1.29	0.69±0.06	0.18±0.03
Myricitrin-treated group	3	2.97±0.15[a]	0.46±0.05[a]	9.98±1.07[a]	0.24±0.02[a]	0.71±0.05[a]
Myricitrin+si-NC group	3	3.01±0.20	0.47±0.04	10.02±1.15	0.23±0.02	0.72±0.08
Myricitrin+si-circZNF292 group	3	1.64±0.10[b]	0.80±0.06[b]	17.29±0.78[b]	0.50±0.05[b]	0.35±0.03[b]
F		163.188	107.321	96.786	85.623	59.310
P		<0.001	<0.001	<0.001	<0.001	<0.001

Note: Compared with respective high glucose group, [a]P<0.05; compared with respective myricitrin+si-NC group, [b]P<0.05 (One-way ANOVA, LSD-t test) siRNA: small interfering RNA; miR: microRNA; bax: bcl-2 associated X protein; bcl-2: B-cell lymphoma-2; siR-NC: small interfering RNA-negative control

2.8 Comparison of MDA concentration and SOD activity among different siRNA transfection groups

There were statistically significant differences in MDA concentration and SOD activity among high glucose group, myricitrin group, myricitrin + siR-NC group and myricitrin + siR-circZNF292 group (F = 49. 375,149.745, all at P < 0.001). Compared with the myricitrin + siR-NC group, MDA concentration was significantly higher, while SOD activity was significantly lower in the myricitrin + siR-circZNF292 group (all at P < 0.05) (Table 7).

Table 7 Comparison of MDA concentration and SOD activity among different siRNA-transfected groups ($\bar{x}\pm s$)

Group	Sample size	MDA (mmol/L)	SOD [μmol/(min·L)]
High glucose group	3	347.23±25.43	48.55 ± 5.99
Myricitrin-treated group	3	159.82±17.15[a]	181.07±10.06[a]
Myricitrin+siR-NC group	3	155.41±19.84	186.12 ± 9.96
Myricitrin+siR-circZNF292 group	3	254.10±25.99[b]	133.69 ± 9.45[b]
F		49.375	149.745
P		<0.001	<0.001

Note: Compared with respective high glucose group, [a]P<0.05; compared with m respective yricitrin+si-NC group, [b]P<0.05 (One-way ANOVA, LSD-t test) siRNA: small interfering RNA; MDA: malondialedhyde; SOD: superoxide dismutase; siR-NC: small interfering RNA-negative control

3 Discussion

DR is one of common ocular microvascular complications of diabetes mellitus. The abnormalities of retinal metabolism under hyperglycemic conditions, promotion of oxidative stress and inflammation contribute to HRMECs dysfunction and apoptosis, ultimately affecting the stability of the structure and function of the blood-retinal barrier. In this regard, the prevention or early treatment of DR is of great significance[19-20].

Myricitrin can promote hypoxia/reoxygenation induced cardiomyocyte proliferation and inhibit cell apoptosis as well as caspase-3 activity, thereby reducing oxidative stress response and cardiomyocyte injury[21]. Myricitrin also inhibits oxidative stress injury and inflammation caused by spinal cord trauma through regulating bcl-2/bax signaling pathway in rats[22]. In the present study, the results showed that high glucose gave rise to an elevated apoptosis rate of HRMECs and expression of bax, but it lowered the level of bcl-2 expression. The apoptosis rate of HRMECs and expression of bax reduced with increasing doses of myricitrin. Conversely, an increase in the expression of bcl-2 proteins was observed in a dose-dependent manner, indicating that myricitrin could inhibit

hyperglycemic induced HRMECs apoptosis. The results also showed that MDA concentration increased while SOD activity decreased in high glucose-induced HRMECs. Conversely, myricitrin was capable of reducing MDA concentration while increasing SOD activity in a dose-dependent manner, suggesting that myricitrin could inhibit the peroxidation damage in high glucose-induced HRMECs. However, the molecular mechanism of myricitrin on high glucose-induced peroxidation damage and apoptotic signaling pathways remains unclear.

CircRNAs are known for their stability, retention and specificity. Some circRNAs sequences are rich in miRNA response elements which can bind and adsorb miRNA to regulate the expression of target genes. In recent years, an increasing number of studies have showed abnormal circRNA expressions in DR and it may serve as a potential target for DR treatment. CircZNF292, a widely studied circRNA, plays an important role in regulating cell apoptosis under oxidative stress. CircZNF292 were abnormally expressed in myocardial H9c2 cells induced by oxygen glucose deprivation and regulate cell proliferation and apoptosis through Wnt3aβ-catenin[23]. Since circZNF292 expression is significantly down-regulated in age-related cataract, up-regulation of circZNF292 expression can inhibit lens epithelial cell apoptosis by competing with miR-23b-3p in regulating the expression of antioxidant genes[13]. In this study, the results showed decreased expressions of circZNF292 and increased expressions of miR-23b-3p in high glucose-induced HRMECs. However, myricitrin was capable of increasing circZNF292 expressions while reducing miR-23b-3p expressions in a concentration dependent manner, suggesting that myricitrin is involved in the regulation of circZNF292/ miR-23b-3p expression. Our results also showed that up-regulation of circZNF292 expressions via transfection could suppress the expressions of miR-23b-3p, which enhances the antioxidant ability and inhibits cell apoptosis in hyperglycemia induced HRMECs. Meanwhile, transfection of siRNA inhibited circZNF292 expressions and enhanced miR-23b-3p expressions, which reversed the ability of anti-apoptosis and antioxidant of myricitrin on hyperglycemia induced HRMECs. The results from the dual luciferase reporter assay demonstrated there was a targeting relationship between circZNF292 and miR-23b-3p in HRMECs. These findings indicate that myricitrin could inhibit miR-23b-3p expressions by up-regulating circZNF292 expressions in high glucose induced HRMECs, which is helpful in enhancing the antioxidant ability of cells and suppressing cell apoptosis. However, further studies are needed to investigate whether myricitrin is involved in the regulation of other genes or signal pathways in DR.

In conclusion, circZNF292 could target miR-23b-3p and regulate its expressions. And the circZNF292/miR-23b-3p molecular axis plays a significant role in regulating oxidative stress injury and cell apoptosis in high glucose induced HRMECs. Myricitrin can inhibit cell apoptosis of high glucose induced HRMECs and enhance their antioxidant ability by promoting circZNF292 expressions and inhibiting miR-23b-3p expressions. These findings provide some experimental basis for treating DR with myricitrin. Its safety and efficacy should be further investigated in animal models of DR.

Conflict of interest None declared.

Author contributions Liu Qian and Dong Yangzeng participated in the designing of the study. Liu Qian and Liu Changgeng performed the experiments. Liu Qian, Liu Changgeng, Li Haijun and Zhang Ying collected and analyzed the data. Liu Qian wrote the manuscript. Liu Qian, Liu Changgeng and Li Haijun revised the manuscript. The manuscript was finalized by Liu Qian and Dong Yangzeng.

References

[1] Xu HY, Cheng JP, Zhang J. The effects of naringenin on oxidative damage, apoptosis and Nrf2-ARE in rats with diabetic retinopathy [J]. J Clin Exp Med, 2020, 19(2):128-132. DOI: 10.3969/j.issn.16714695.2020.02.005.

[2] Cui XM, Wang S, Xu SJ, et al. Effect of resveratrol on the proliferation of human retinal capillary endothelial cells induced by high glucose and its possible mechanism [J]. J Shandong Univ (Health Sci), 2019, 57(3):19-24. DOI: 10.6040/j.issn.1671-7554.0.2018.799.

[3] Cui J, Gong R,Hu S, et al. Gambogic acid ameliorates diabetes-induced proliferative retinopathy through inhibition of the HIF-la/VEGF expression via targeting PI3K/AKT pathway [J]. Life Sci, 2018,192: 293-303. DOI.10.1016/j.lfs.2017.11.007.

[4] Cai ZB, Tao K, Wang B, et al. Myricitrin attenuated MPP^+ -induced apoptosis in SN4741 cells by inhibiting mitochondrial dysfunction [J]. Chin J Neuroanat, 2015, 31(5):579-583. DOI: 10.16557/10007547.201505008.

[5] Zhang XJ, Hou Z, Bai XY, et al. Studies on myricetin inducing human hepatoma HepG-2 cells apoptosis through signal transduction pathway [J]. Chin Pharmacol Bull, 2014, 30(1):71-76. DOI: 10.3969/j.issn.1001-1978.2014.01.016.

[6] Kim DY, Kim SR, Jung UJ. Myricitrin ameliorates hyperglycemia, glucose intolerance, hepatic steatosis, and inflammation in high-fat diet/ streptozotocin-induced diabetic mice [J/OL]. Int J Mol Sci, 2020, 21(5): 1870 [2021-06-12]. http://www.ncbi.nlm.nih.gov/puhmed/32182914. DOI: 10.3390/ijms21051870.

[7] Ahangarpour A, Oroojan AA, Khorsandi L, et al. Antioxidant effect of myricitrin on hyperglycemia-induced oxidative stress in C2C12 cell [J]. Cell Stress Chaperones, 2018, 23(4):773-781. D01: 10.1007/sl2192-018-0888-z.

[8] Arumugam B, Palanisamy UD, Chua KH, et al. Protective effect of myricetin derivatives from Syzygium malaccense against hydrogen peroxide-induced stress in ARPE-19 cells [J]. Mol Vis, 2019, 25:47-59.

[9] Qiao Y,Fan CL,Tang MK. Astragaloside IV protects rat retinal capillary endothelial cells against high glucose-induced oxidative injury [J] . Drug Des Devel Ther, 2017, 11:3567-3577. DOI: 10.2147/DDDT. SI52489.

[10] Zhu K, Hu X, Chen H, et al. Downregulation of circRNA DMNT3B contributes to diabetic retinal vascular dysfunction through targeting miR-20b-5p and BAMBI [J]. EBioMedicine, 2019, 49:341-353. DOI: 10.1016/j.ebiom.2019.10.004.

[11] Liu G, Zhou S , Li X, et al. Inhibition of hsa_circ_0002570 suppresses high-glucose-induced angiogenesis and inflammation in retinal microvascular endothelial cells through miR-i243/angiomotin axis[J]. Cell Stress Chaperones, 2020, 25(5):767-777. DOI: 10.1007/S12192-020-01111-2.

[12] Xu X, Gao R,Li S, et al. Circular RNA circZNF292 regulates H_2O_2- induced injury in human lens epithelial HLE-B3 cells depending on the regulation of the miR-222-3p/E2F3 axis [J] . Cell Biol Int, 2021, 45(8):1757-1767. DOI: 10.1002/chin.11615.

[13] Liang S,Dou S, Li W, et al. Profiling of circular RNAs in age-related cataract reveals circZNF292 as an antioxidant by sponging miR-23b-3p [J/OL]. Aging (Albany NY) , 2020, 12(17):17271-17287 [202106-16]. http://www.ncbi.nlm.nih.gov/puhmed/32913142. DOI: 10.18632/aging. 103683.

[14] Zhao S, Li T, Li J, et al. miR-23b-3p induces the cellular metabolic memory of high glucose in diabetic retinopathy through a SIRT1- dependent signalling pathway [J]. Diabetologia, 2016, 59(3):644-654. DOI: 10.1007/s00125-015-3832-0.

[15] Cao F, Lyu X, Dong KF, et al. AMG-102 inhibits proliferation and induces apoptosis of laryngeal squamous cell carcinoma cells by regulating c-Met/P13K/Akt pathway [J]. Chin J Oncol, 2020, 42(2):99-104. DOI: 10.3760/cma.j.issn.0253-3766.2020.02.003.

[16] Zhou YD, Jiang W, Zhou P. Scutellarin affects LPS-induced oxidative stress and apoptosis of glomerular epithelial cells by up-regulating miR-7-5p[J]. Chin J Pathophysiol, 2020, 36(10):1860-1866. DOI: 10. 3969/j.issn.1000-4718.2020.10.018.

[17] Liu ZL,Lu YY. Effects of IncRNA FLVCR1-AS1 targeting miR- 381-3p on proliferation and apoptosis of colorectal cancer cells and molecular mechanism [J]. Shandong Med J, 2020, 60(29):5-9. DOI: 10. 3969/j.issn.1002-266X.2020.29.002.

[18] Gao F, Wu ZP, Ruan YH. Inhibitory effect of miR-146a on high glucose-induced apoptosis of retinal microvascular endothelial cells and its mechanism [J]. Chin J Exp Ophthalmol, 2021, 39(5):398-403. DOI: 10.3760/cma.j.cnll5989-20190703-00286.

[19] Ren Q, Li H, Wang X. The circular RNA ZNF292 alleviates OGD- induced injury in H9c2 cells via targeting BNIP3 [J]. Cell Cycle, 2019, 18(23):3365-3377. DOI: 10.1080/15384101.2019.1676585.

[20] Fang MY, Li QM, Yang X, et al. Protective effect of asiatic acid on blood-retinal barrier in diabetic rats [J]. Chin J Exp Ophthalmol, 2021, 39(7):593-601. DOI: 10.3760/cma.j.cnll5989-20201024-00713.

[21] Wang M, Sun GB, Du YY, et al. Myricitrin protects cardiomyocytes from hypoxia/reoxygenation injury: involvement of heat shock protein 90 [J/OL]. Front Pharmacol, 2017,8: 353 [2021-07-18]. DOI: 10.3389/fphar.2017.00353.

[22] Lei Y. Myricitrin decreases traumatic injury of the spinal cord and exhibits antioxidant and anti-inflammatory activities in a rat model via inhibition of COX-2, TGF-β1, p53 and elevation of Bcl-2/Bax signaling pathway [J]. Mol Med Rep, 2017, 16(5):7699-7705. DOI: 10.3892/mmr.2017.7567.

[23] Gu S, Zhan PF, Wang WJ, et al. Inhibitory effects of miR-146a on retinal inflammation induced by high glucose in human retinal endothelial cells [J]. Chin J Exp Ophthalmol, 2020, 38(9):733-739. DOI: 10.3760/cma.j.cnll5989-20190213-00051.